# Non-Quasi-Geostrophic Effects in Baroclinic Waves with Latent Heat Release

CHUNG-MUH TANG[1] AND GEORGE H. FICHTL

*Systems Dynamics Laboratory, NASA/Marshall Space Flight Center, Huntsville, AL 35812*

(Manuscript received 16 May 1983, in final form 6 February 1984)

ABSTRACT

A second-order theory of baroclinic waves is developed to investigate non-quasi-geostrophic behavior in disturbances in which latent heat release associated with condensation is permitted to occur in an atmosphere saturated with water vapor. A two-level formulation without $\beta$-effect is used to analyze these disturbances. The analysis involves an expansion of the flow into a basic state zonal flow with superimposed perturbation which is assumed to be independent of the meridional direction. The superimposed perturbation consists of linear combination of a quasi-geostrophic contribution and a non-quasi-geostrophic departure. The basic state flow with the superimposed quasi-geostrophic perturbation has been investigated by the authors in a previous paper. The governing equations for the non-quasi-geostrophic contribution consist of a nonlinear (thermodynamic) integro-differential equation and a nonhomogeneous (vorticity) differential equation. The nonlinearity is a direct result of latent heat release associated with pseudo-adiabatic ascent; i.e., saturated ascending air parcels and dry descending air parcels. The nonhomogeneity arises from the non-quasi-geostrophic terms in the vorticity equation. In this theory we use the quasi-geostrophic contribution to calculate the non-quasi-geostrophic terms which generate the second-order solution.

The problem is characterized by two parameters, namely a rotational Froude number $F = 2f^2(S_d p_2^2 k_d^2)^{-1}$ (where $f$ is the Coriolis parameter, $S_d$ the static stability in descending portion of the wave, $p_2$ the pressure at the middle level, and $k_d = \pi/b$, $b$ being the horizontal extent of the descending or dry portion of the wave) and a moisture parameter $\epsilon$ which is proportional to the midlevel vertical gradient of mean flow specific humidity. For $\epsilon \neq 0$ the disturbances are characterized by $a/b \neq 1$, where $a$ is the horizontal extent of the ascending or wet portion of the wave. The quasi-geostrophic contribution to the disturbance is characterized by two modes for $F > 1$. The first mode has a narrow region of strong ascending motion and a wide region of weak descending motion ($a/b < 1$), with the reverse for the second mode ($a/b > 1$). These solutions, developed by the authors in an earlier paper, are used to calculate the non-quasi-geostrophic solution terms mentioned above.

For the first moist mode, due to the non-quasi-geostrophic effects, both the trough and ridge are intensified at the upper level with stronger intensification of the trough and are weakened at the lower level with considerable weakening of the ridge. The formation of the frontal zone on the east side of the descending region is a feature similar to that in the dry model with non-quasi-geostrophic effects. For the second moist mode, due to the non-quasi-geostrophic effects, both trough and ridge are weakened at the upper level, but they are intensified at the lower level. The temperature profile in each region is nearly symmetric. The total vertical motion field is asymmetric in each region for both the first and second moist modes.

The main characteristics of the energetics are described by the transports due to the first-order eddy. The transports due to the second-order eddy have only minor influence except for large $F$ such as $F \geq 10$ for the first mode and except for $\epsilon$ near unity for the second mode.

## 1. Introduction

Saltzman and Tang (1972, 1974, 1975; hereafter referred to as ST) developed a second-order, non-quasi-geostrophic baroclinic wave theory which can reproduce the features observed on weather maps, including 1) the poleward and eastward displacements of the intensifying cyclonic circulation systems (lows), 2) the equatorward and eastward displacements of the more diffuse anticyclonic circulation systems (highs) in low levels, 3) the formation of a cutoff low aloft with a "splitting" of the jet stream, 4) the development of an S-shaped frontal zone, and 5) the development of a "bow-shaped" descending region south of the surface low center with the accompanying "comma-shaped" rising region which resembles the comma-shaped cloud region frequently observed on satellite pictures. However, the effects of latent heat release were excluded in the model.

Recently Tang and Fichtl (1983; hereafter referred to as TF) developed a quasi-geostrophic baroclinic wave theory to study the effects of latent heat release with disturbances assumed to be independent of the meridional coordinate. TF used the two-level, quasi-geostrophic model (Phillips, 1954) without $\beta$-effect for an atmosphere initially saturated with water vapor and subject to pseudo-adiabatic lifting and dry adiabatic

[1] Visiting Scientist from Universities Space Research Association, The American City Building, Suite 311, Columbia, MD 21044.

subsidence. Thus, each region was characterized by constant but different static stability. This results in a static stability–vertical velocity correlation which produces mean uniform heating with an attendant increase in thickness. The horizontal extent of the disturbance in each region is permitted to be different. A set of integro-differential equations is developed for a perturbation superimposed on a mean zonal flow with vertical wind shear constant in space and time. The resulting equations are solved in the ascending and descending portions of the wave separately and have solutions which look like the classical two layer ones described by Holton (1972). The mass continuity constraint demands that the growth rates in the rising and sinking portions of the wave be equal, so that the ratio of the horizontal dimensions of the ascending and descending portions of the wave is related to the ratio of static stability in each region and a rotational Froude number for the dry or descending portion of the wave. Interfacial conditions (continuity of height and temperature fields) were used to match the solutions at the interface between the ascending and descending portions of the wave to permit a study of the structure of the wave. An analysis of the energetics showed the presence of a latent heat release term which contributes directly to the generation of eddy available potential energy. Although this term is small compared to the vertical and horizontal heat transports, latent heat release caused a significant change in the structure of the waves such that large departure occurred in the horizontal heat transport from dry atmospheric values.

In order to study how the effects of latent heat release are manifest in the non-quasi-geostrophic terms, we extend the model of TF by considering the small amplitude wave disturbance in that paper and designating it as the first-order solution and substituting it into the non-quasi-geostrophic terms to generate the second-order solution. In this formulation, we assume that the disturbance has no meridional variation, so that some of the features produced in ST will not be reproduced here; however, we expect to see the effects of latent heat release on the relative strength of the trough and ridge, the generation of frontal zones, and the evolution of the vertical motion field.

## 2. Formulation of the two-level model

Consider the two-level model in which we apply the vorticity equation at level 1 ($p_1 = 250$ mb) and at level 3 ($p_3 = 750$ mb) and apply the thermodynamic energy equation at level 2 ($p_2 = 500$ mb), with vanishing vertical velocity at the top and bottom, $\omega_0 = \omega_4 = 0$. They are

$$\frac{\partial}{\partial t}\nabla^2\psi_1 + J(\psi_1, \nabla^2\psi_1) = \frac{f}{p_2}\omega_2 + H_1, \quad (1a)$$

$$\frac{\partial}{\partial t}\nabla^2\psi_3 + J(\psi_3, \nabla^2\psi_3) = -\frac{f}{p_2}\omega_2 + H_3, \quad (1b)$$

$$\frac{\partial}{\partial t}T_2 + J(\psi_2, T_2) - \frac{p_2}{R}S\omega_2 = -\left(u_{\chi 2}\frac{\partial}{\partial x} + v_{\chi 2}\frac{\partial}{\partial y}\right)T = 0, \quad (1c)$$

$$\frac{\partial u_{\chi 1}}{\partial x} + \frac{\partial v_{\chi 1}}{\partial y} = \frac{\omega_2}{p_2}, \quad \frac{\partial u_{\chi 3}}{\partial x} + \frac{\partial v_{\chi 3}}{\partial y} = -\frac{\omega_2}{p_2}, \quad (1d, e)$$

in which

$$H = -\left(u_\chi\frac{\partial}{\partial x} + v_\chi\frac{\partial}{\partial y}\right)\zeta - \omega\frac{\partial\zeta}{\partial p} + \zeta\frac{\partial\omega}{\partial p} + \frac{\partial\omega}{\partial y}\frac{\partial u}{\partial p} - \frac{\partial\omega}{\partial x}\frac{\partial v}{\partial p}, \quad (2)$$

where $\zeta = \nabla^2\psi$. The symbols have their usual meanings except for $S$.

The quantity $S$ is defined as

$$S = S_d(1 - \delta\epsilon) \quad (3)$$

in which the moisture parameter is given by

$$\epsilon = \frac{R}{S_d p_2}\frac{L}{C_p}\left(\frac{\partial q_s}{\partial p}\right)_2, \quad (4)$$

$$\delta = \begin{cases} 1, & \omega_2 < 0 \\ 0, & \omega_2 \geq 0. \end{cases} \quad (5)$$

The subscripts 2 and $T$ relate to the subscripts 1 and 3 as follows:

$$\left.\begin{aligned} (\ )_2 &= [(\ )_1 + (\ )_3]/2 \\ (\ )_T &= [(\ )_1 - (\ )_3]/2 \end{aligned}\right\}. \quad (6)$$

The non-quasi-geostrophic terms in (1c) vanish because $\chi_2 = 0$.

A small amplitude disturbance (denoted by a prime), which has no variation in the meridional ($y$) direction, is superimposed on a basic mean zonal flow with vertical shear constant in space and time in an atmosphere saturated with water vapor. A frame of reference is taken which translates with the mean zonal wind at the middle level. This permits use of the transformation of coordinates

$$\left.\begin{aligned} x_0 &= x - \bar{u}_2 t \\ t_0 &= t \end{aligned}\right\}, \quad (7)$$

where $x_0$ and $t_0$ are the zonal and time coordinates in the moving frame of reference. The bar denotes a zonal average over a single wave and is defined by

$$(\bar{\ }) = \lim_{\Delta\to 0}\frac{1}{a+b}\left(\int_{-a+\Delta}^{0}(\tilde{\ })dx_1 + \int_0^{\Delta}(\hat{\ })dx_0 + \int_{\Delta}^{b}(\hat{\ })dx_0 + \int_b^{b+\Delta}(\tilde{\ })dx_0\right), \quad (8)$$

where the tilde indicates the quantity in the pseudo-adiabatically ascending region with horizontal extent

$a$, and the caret indicates that in the dry-adiabatically descending region with the horizontal extent $b$. In contrast to the classical "dry" model, disturbances characterized by $a \neq b$ are allowed. The increment $\Delta$ is introduced in (8) because the quantity represented by the parentheses may be discontinuous at the vertical interfaces between the pseudo-adiabatically ascending region and dry adiabatically descending region.

Using (7),

$$\left.\begin{aligned}\frac{\partial}{\partial t_0} &= \frac{\partial}{\partial t} + \bar{u}_2 \frac{\partial}{\partial x} \\ \frac{\partial}{\partial x_0} &= \frac{\partial}{\partial x}\end{aligned}\right\}. \tag{9}$$

Since the disturbance has no meridional variation,

$$f\psi = \Phi. \tag{10}$$

Combination of (10) and the hydrostatic relation yields

$$T_2 = \frac{2f}{R}\psi_T. \tag{11}$$

Using (9) and substituting (11) in (1c) together with (1d, e),

$$\left(\frac{\partial}{\partial t_0} + \bar{u}_T \frac{\partial}{\partial x_0}\right)\frac{\partial^2 \psi_1'}{\partial x_0^2} = \frac{f}{p_2}\omega_2' + H_1', \tag{12a}$$

$$\left(\frac{\partial}{\partial t_0} - \bar{u}_T \frac{\partial}{\partial x_0}\right)\frac{\partial^2 \psi_3'}{\partial x_0^2} = -\frac{f}{p_2}\omega_2' + H_3', \tag{12b}$$

$$\frac{\partial}{\partial t_0}\psi_T + v_{\psi 2}\frac{\partial}{\partial y}\psi_T - \frac{p_2 S}{2f}\omega_2 = 0, \tag{12c}$$

$$\frac{\partial u_{x1}'}{\partial x_0} = \frac{\omega_2'}{p_2}, \quad \frac{\partial u_{x3}'}{\partial x_0} = -\frac{\omega_2'}{p_2}. \tag{12d, e}$$

To write the functions $H_1'$ and $H_3'$ explicitly, $\omega$ must be known at levels 1 and 3 in terms of the value at level 2. A parabolic profile is used for $\omega$, i.e.,

$$\omega = \omega_2 \frac{p}{p_2}\left(2 - \frac{p}{p_2}\right). \tag{13}$$

Applying (13) at levels 1 and 3,

$$\omega_1 = \omega_3 = \frac{3}{4}\omega_2. \tag{14}$$

Next (12c), which is exactly the same as (11c) in TF, is considered. This equation provides the mechanism for latent heat release to effect the dynamic behavior of the baroclinic wave via horizontal variation of static stability across the interface between the ascending and descending portions of the wave. The developments in TF from (11c) to (17a, b) concerning the definition of the basic state static stability, static stability perturbations, static stability-vertical velocity correlations, and associated basic state $\psi_T$ field remain valid. Thus, the application of the horizontal averaging operator (8) to (12c) yields a relationship between the local change of $\psi_T$ and the static stability-vertical velocity correlation, namely $\overline{S'\omega'}$. Furthermore, $S'$ in the ascending and descending portions of the wave are constants but have different values in each portion of the wave, i.e., $\hat{S}' = -(a/b)\tilde{S}' = a\epsilon S_d/(a+b)$. Accordingly, the $\overline{S'\omega'}$ correlation can be readily calculated in terms of the average vertical velocity over the ascending or descending portions of the wave. Thus, the mass continuity equation permits $\overline{S'\omega'}$ to be written exclusively in terms of an integral of $\tilde{\omega}_2$ over the moist region or an integral of $\hat{\omega}_2$ over the dry region. Accordingly, (12c) is written in TF as follows

$$\bar{\psi}_T = -\bar{u}_T y - \frac{p_2 S_d \epsilon}{2f(a+b)} \times \int_0^{t_0}\int_{-a}^{0} \tilde{\omega}_2' dx_0 dt_0 + \text{constant}. \tag{15}$$

This equation shows that the diabatic heating due to the latent heat release in the moist ascending region results in mean zonal heating. Application of (15) to (12c) permits the perturbation equations to be written separately for the descending and ascending regions as follows:

Descending region;

$$\left(\frac{\partial}{\partial t_0} + \bar{u}_T \frac{\partial}{\partial x_0}\right)\frac{\partial^2 \hat{\psi}_1'}{\partial x_0^2} = \frac{f}{p_2}\hat{\omega}_2' + \hat{H}_1', \tag{16a}$$

$$\left(\frac{\partial}{\partial t_0} - \bar{u}_T \frac{\partial}{\partial x_0}\right)\frac{\partial^2 \hat{\psi}_3'}{\partial x_0^2} = -\frac{f}{p_2}\hat{\omega}_2' + \hat{H}_3', \tag{16b}$$

$$\frac{\partial}{\partial t_0}\hat{\psi}_T' - \bar{u}_T \frac{\partial}{\partial x_0}\hat{\psi}_2' - \frac{p_2}{2f}S_d\left[\hat{\omega}_2' - \frac{\epsilon}{a+b}\int_0^b \hat{\omega}_2' dx_0\right] = 0, \tag{16c}$$

$$\frac{\partial \hat{u}_{x1}'}{\partial x_0} = \frac{\hat{\omega}_2'}{p_2}, \quad \frac{\partial \hat{u}_{x3}'}{\partial x_0} = -\frac{\hat{\omega}_2'}{p_2}. \tag{16d, e}$$

Ascending region;

$$\left(\frac{\partial}{\partial t_0} + \bar{u}_T \frac{\partial}{\partial x_0}\right)\frac{\partial^2 \tilde{\psi}_1'}{\partial x_0^2} = \frac{f}{p_2}\tilde{\omega}_2' + \tilde{H}_1', \tag{17a}$$

$$\left(\frac{\partial}{\partial t_0} - \bar{u}_T \frac{\partial}{\partial x_0}\right)\frac{\partial^2 \tilde{\psi}_3'}{\partial x_0^2} = -\frac{f}{p_2}\tilde{\omega}_2' + \tilde{H}_3', \tag{17b}$$

$$\frac{\partial}{\partial t_0}\tilde{\psi}_T' - \bar{u}_T \frac{\partial}{\partial x_0}\tilde{\psi}_2' - \frac{p_2 S_d}{2f} \times \left[(1-\epsilon)\tilde{\omega}_2' + \frac{\epsilon}{a+b}\int_{-a}^{0}\tilde{\omega}_2' dx_0\right] = 0, \tag{17c}$$

$$\frac{\partial \tilde{u}_{x1}'}{\partial x_0} = \frac{\tilde{\omega}_2'}{p_2}, \quad \frac{\partial \tilde{u}_{x3}'}{\partial x_0} = -\frac{\tilde{\omega}_2'}{p_2} \tag{17d, e}$$

in which

$$H'_1 = \left[\frac{5}{2p_2}\left(\omega'_2\frac{\partial^2\psi'_T}{\partial x_0^2}\right) + \frac{1}{p_2}\left(\omega'_2\frac{\partial^2\psi'_2}{\partial x_0^2}\right) + \frac{3}{2p_2} \times \left(\frac{\partial\omega'_2}{\partial x_0}\frac{\partial\psi'_T}{\partial x_0}\right) - \left(u'_{x1}\frac{\partial^3\psi'_2}{\partial x_0^3}\right) - \left(u'_{x1}\frac{\partial^3\psi'_T}{\partial x_0^2}\right)\right]', \quad (18a)$$

$$H'_3 = \left[\frac{5}{2p_2}\left(\omega'_2\frac{\partial^2\psi'_T}{\partial x_0^2}\right) - \frac{1}{p_2}\left(\omega'_2\frac{\partial^2\psi'}{\partial x_0^2}\right) + \frac{3}{2p_2} \times \left(\frac{\partial\omega'_2}{\partial x_0}\frac{\partial\psi'_T}{\partial x_0}\right) + \left(u'_{x1}\frac{\partial^3\psi'_2}{\partial x_0^3}\right) - \left(u'_{x1}\frac{\partial^3\psi'_T}{\partial x_0^3}\right)\right]'. \quad (18b)$$

From the continuity equation we have the mass continuity integral constraint

$$\int_{-a}^{0}\tilde{\omega}_2 dx_0 + \int_0^b \hat{\omega}_2 dx_0 = 0, \quad (19)$$

which implies that the vertical motion vanishes when zonally averaged over a single wave or multiples of waves.

Equations (16a)–(19) along with (15) provide the basic set of equations for the analysis that follows. A number of features are worth noting. The first is a set of integro-differential equations wherein the integrals in (16c) and (17c) are a direct result of the release of latent heat in the moist ascending region. This shows that latent heat release in a global context affects the local behavior of the wave. Second, these equations have two kinds of nonlinearities. In the first kind, the traditional one is manifested by the presence of $H'_1$ and $H'_3$ in the equations. The other kind, excluding $H'_1$ and $H'_3$, results from the fact that, despite the $\psi$'s and $\omega'_2$ occurring in a linear way individually in (16c) and (17c), these equations are nonlinear when taken together because the form of thermodynamic energy equation changes when passing from the moist region to the dry region. This is a result of the static stability variation across the interface between ascending and descending portions of the wave.

Finally, it should be noted that the $\bar{\psi}_T$ field can be expressed in terms of the average vertical velocity across the ascending or descending portions of the wave via the mass continuity constraint (19).

## 3. Expansion of the equations

Each dependent variable is decomposed as follows:

$$\xi = \bar{\xi} + \xi', \quad (20a)$$

$$\bar{\xi} = \bar{\xi}^{(0)} + \bar{\xi}^{(1)} + \bar{\xi}^{(2)}, \quad (20b)$$

$$\xi' = \xi^{(1)} + \xi^{(2)}. \quad (20c)$$

For the perturbation field, $\xi^{(1)}$ is defined as the first-order solution which satisfies the quasi-geostrophic version of the governing equations which determine the stability of the basic zonal current $\bar{u}^{(0)}$. The $\xi^{(2)}$ variables represent the second-order eddy field generated through the non-quasi-geostrophic terms due to the amplifying $\xi^{(1)}$ field. The quantities $\bar{\xi}^{(1)}$ and $\bar{\xi}^{(2)}$ are the zonally averaged first-order and second-order fields, respectively.

The zonally averaged temperature field is expressed in (15). The basic (zero-order) field, first-order, and second-order fields are respectively

$$\bar{\psi}_T^{(0)} = -\bar{u}_T^{(0)}y + \text{constant}, \quad (21a)$$

$$\bar{\psi}_T^{(1)} = -\frac{p_2 S_d \epsilon}{2f(a+b)}\int_0^{t_0}\int_{-a}^{0}\tilde{\omega}_2^{(1)}dx_0dt_0, \quad (21b)$$

$$\bar{\psi}_T^{(2)} = -\frac{p_2 S_d \epsilon}{2f(a+b)}\int_0^{t_0}\int_{-a}^{0}\tilde{\omega}_2^{(2)}dx_0dt_0. \quad (21c)$$

It is noted from (21b) that the first-order zonal effect of the latent heat release is to increase the zonally averaged temperature (cf. TF). Differentiating (21a, b, c) with respect to $y$,

$$\bar{u}_T^{(0)} = -\frac{\partial}{\partial y}\bar{\psi}_T^{(0)}, \quad (22a)$$

$$\bar{u}_T^{(1)} = \bar{u}_T^{(2)} = 0. \quad (22b)$$

The first-order and second-order zonal wind shear vanish individually because the perturbation fields have no meridional ($y$) variation. Therefore, in this formulation the vertical shear of the mean zonal wind remains constant, and is equal to the basic-state shear.

Substitution of the above expressions in (16) and (17) yields the following:

1) First-order eddy equations

Descending region;

$$\left(\frac{\partial}{\partial t_0} + \bar{u}_T^{(0)}\frac{\partial}{\partial x_0}\right)\frac{\partial^2\hat{\psi}_1^{(1)}}{\partial x_0^2} = \frac{f}{p_2}\hat{\omega}_2^{(1)}, \quad (23a)$$

$$\left(\frac{\partial}{\partial t_0} - \bar{u}_T^{(0)}\frac{\partial}{\partial x_0}\right)\frac{\partial^2\hat{\psi}_3^{(1)}}{\partial x_0^2} = -\frac{f}{p_2}\hat{\omega}_2^{(1)}, \quad (23b)$$

$$\frac{\partial}{\partial t_0}\hat{\psi}_T^{(1)} - \bar{u}_T^{(0)}\frac{\partial}{\partial x_0}\hat{\psi}_2^{(1)} - \frac{p_2}{2f}S_d\left[\hat{\omega}_2^{(1)} - \frac{\epsilon}{a+b}\int_0^b\hat{\omega}_2^{(1)}dx_0\right] = 0, \quad (23c)$$

$$\frac{\partial\hat{u}_{x1}^{(1)}}{\partial x_0} = \frac{\hat{\omega}_2^{(1)}}{p_2}, \quad \frac{\partial\hat{u}_{x3}^{(1)}}{\partial x_0} = -\frac{\hat{\omega}_2^{(1)}}{p_2}. \quad (23d, e)$$

Ascending region;

$$\left(\frac{\partial}{\partial t_0} + \bar{u}_T^{(0)}\frac{\partial}{\partial x_0}\right)\frac{\partial^2\tilde{\psi}_1^{(1)}}{\partial x_0^2} = \frac{f}{p_2}\tilde{\omega}_2^{(1)}, \quad (24a)$$

$$\left(\frac{\partial}{\partial t_0} - \bar{u}_T^{(0)}\frac{\partial}{\partial x_0}\right)\frac{\partial^2\tilde{\psi}_3^{(1)}}{\partial x_0^2} = -\frac{f}{p_2}\tilde{\omega}_2^{(1)}, \quad (24b)$$

$$\frac{\partial}{\partial t_0}\tilde{\psi}_T^{(1)} - \bar{u}_T^{(0)}\frac{\partial}{\partial x_0}\tilde{\psi}_2^{(1)} - \frac{p_2}{2f}S_d \times\left[(1-\epsilon)\tilde{\omega}_2^{(1)} + \frac{\epsilon}{a+b}\int_{-a}^{0}\tilde{\omega}_2^{(1)}dx_0\right] = 0, \quad (24c)$$

$$\frac{\partial \tilde{u}_{x_1}^{(1)}}{\partial x_0} = \frac{\tilde{\omega}_2^{(1)}}{p_2}, \quad \frac{\partial \tilde{u}_{x_3}^{(1)}}{\partial x_0} = -\frac{\tilde{\omega}_2^{(1)}}{p_2}. \quad (24d, e)$$

2) Second-order eddy equations

Descending region;

$$\left(\frac{\partial}{\partial t_0} + \bar{u}_T^{(0)}\frac{\partial}{\partial x_0}\right)\frac{\partial^2\hat{\psi}_1^{(2)}}{\partial x_0^2} = \frac{f}{p_2}\hat{\omega}_2^{(2)} + \hat{H}_1^{(a)}, \quad (25a)$$

$$\left(\frac{\partial}{\partial t_0} - \bar{u}_T^{(0)}\frac{\partial}{\partial x_0}\right)\frac{\partial^2\hat{\psi}_3^{(2)}}{\partial x_0^2} = -\frac{f}{p_2}\hat{\omega}_2^{(2)} + \hat{H}_3^{(a)}, \quad (25b)$$

$$\frac{\partial}{\partial t_0}\hat{\psi}_T^{(2)} - \bar{u}_T^{(0)}\frac{\partial}{\partial x_0}\hat{\psi}_2^{(2)} - \frac{p_2}{2f}S_d\left[\hat{\omega}_2^{(2)} - \frac{\epsilon}{a+b}\int_0^b\hat{\omega}_2^{(2)}dx_0\right] = 0, \quad (25c)$$

$$\frac{\partial \hat{u}_{x_1}^{(2)}}{\partial x_0} = \frac{\hat{\omega}_2^{(2)}}{p_2}, \quad \frac{\partial \hat{u}_{x_3}^{(2)}}{\partial x_0} = -\frac{\hat{\omega}_2^{(2)}}{p_2}. \quad (25d, e)$$

Ascending region;

$$\left(\frac{\partial}{\partial t_0} + \bar{u}_T^{(0)}\frac{\partial}{\partial x_0}\right)\frac{\partial^2\tilde{\psi}_1^{(2)}}{\partial x_0^2} = \frac{f}{p_2}\tilde{\omega}_2^{(2)} + \tilde{H}_1^{(a)}, \quad (26a)$$

$$\left(\frac{\partial}{\partial t_0} - \bar{u}_T^{(0)}\frac{\partial}{\partial x_0}\right)\frac{\partial^2\tilde{\psi}_3^{(2)}}{\partial x_0^2} = -\frac{f}{p_2}\tilde{\omega}_2^{(2)} + \tilde{H}_3^{(a)}, \quad (26b)$$

$$\frac{\partial}{\partial t_0}\tilde{\psi}_T^{(2)} - \bar{u}_T^{(0)}\frac{\partial}{\partial x_0}\tilde{\psi}_2^{(2)} - \frac{p_2}{2f}S_d \times\left[(1-\epsilon)\tilde{\omega}_2^{(2)} + \frac{\epsilon}{a+b}\int_{-a}^{0}\tilde{\omega}_2^{(2)}dx_0\right] = 0, \quad (26c)$$

$$\frac{\partial \tilde{u}_{x_1}^{(2)}}{\partial x_0} = \frac{\tilde{\omega}_2^{(2)}}{p_2}, \quad \frac{\partial \tilde{u}_{x_3}^{(2)}}{\partial x_0} = -\frac{\tilde{\omega}_2^{(2)}}{p_2}, \quad (26d, e)$$

where

$$H_1^{(a)} = \left[\frac{5}{2p_2}\left(\omega_2^{(1)}\frac{\partial^2\psi_T^{(1)}}{\partial x_0^2}\right) + \frac{1}{p_2}\left(\omega_2^{(1)}\frac{\partial^2\psi_2^{(1)}}{\partial x_0^2} + \frac{3}{2p_2}\left(\frac{\partial\omega_2^{(1)}}{\partial x_0}\frac{\partial\psi_T^{(1)}}{\partial x_0}\right) - \left(u_{x_1}^{(1)}\frac{\partial^3\psi_2^{(1)}}{\partial x_0^3}\right) - \left(u_{x_1}^{(1)}\frac{\partial^3\psi_T^{(1)}}{\partial x_0^3}\right)\right]', \quad (27a)$$

$$H_3^{(a)} = \left[\frac{5}{2p_2}\left(\omega_2^{(1)}\frac{\partial^2\psi_T^{(1)}}{\partial x_0^2}\right) - \frac{1}{p_2}\left(\omega_2^{(1)}\frac{\partial^2\psi_2^{(1)}}{\partial x_0^2} + \frac{3}{2p_2}\left(\frac{\partial\omega_2^{(1)}}{\partial x_0}\frac{\partial\psi_T^{(1)}}{\partial x_0}\right) + \left(u_{x_1}^{(1)}\frac{\partial^3\psi_2^{(1)}}{\partial x_0^3}\right) - \left(u_{x_1}^{(1)}\frac{\partial^3\psi_T^{(1)}}{\partial x_0^3}\right)\right]', \quad (27b)$$

with caret and tilde to each dependent variable to obtain $\hat{H}^{(a)}$ and $\tilde{H}^{(a)}$.

## 4. Time limit of applicability

In this formulation, *a priori* the width of the descending region $b$ has been specified. Then from the stability analysis $a/b$ is determined (cf. TF). Therefore the following conditions must be satisfied

$$\hat{\omega}_2^{(1)} + \hat{\omega}_2^{(2)} > 0, \quad (28a)$$

$$\tilde{\omega}_2^{(1)} + \tilde{\omega}_2^{(2)} < 0, \quad (28b)$$

where

$$\hat{\omega}_2^{(1)} = A_d e^{\nu t_0}\sin k_d x_0, \quad 0 \leqslant x_0 \leqslant b, \quad k_d = \pi/b, \quad A_d > 0, \quad (29a)$$

$$\tilde{\omega}_2^{(1)} = A_m e^{\nu t_0}\sin k_m x_0, \quad -a \leqslant x_0 \leqslant 0, \quad k_m = \pi/a, \quad A_m > 0, \quad (29b)$$

$$\hat{\omega}_2^{(2)} = \hat{\Omega} e^{2\nu t_0}\sin 2k_d x_0, \quad (30a)$$

$$\tilde{\omega}_2^{(2)} = \tilde{\Omega} e^{2\nu t_0}\sin 2k_m x_0, \quad (30b)$$

in which $\hat{\Omega}$ and $\tilde{\Omega}$ are constants and $\nu$ is the growth rate. In view of (29a, b) and (30a, b), in each region the absolute value of the maximum slope of the second-order eddy vertical motion field must be less than that of the first-order eddy vertical motion field. These constraints lead to

$$t_0 < \frac{1}{\nu}\ln\frac{A_d}{2\hat{\Omega}}, \quad (31a)$$

$$t_0 < \frac{1}{\nu}\ln\frac{A_m}{2\tilde{\Omega}}. \quad (31b)$$

Both (31a, b) must be satisfied. Then these give the smaller of the right side in (31a, b) as the upper bound in time, beyond which the solutions are invalid.

## 5. Wave structure and forced zonal mean temperature field

The typical atmospheric parameters at middle latitudes are prescribed as

$f = 1.03 \times 10^{-4}\ \mathrm{s}^{-1}$ at 45° latitude

$S_d = 0.028\ \mathrm{m^2\ s^{-2}\ mb^{-2}}$

$p_2 = 500\ \mathrm{mb}$

$\bar{u}_T^{(0)} = 8\ \mathrm{m\ s^{-1}}$

$A_d = 0.35 \times 10^{-3}\ \mathrm{mb\ s^{-1}}$

$F = 1 + \sqrt{2}$ (most unstable wave).

The amplitude of the vertical motion in the descending region at the middle level, as given by $A_d$, corresponds to about 0.5 cm $\mathrm{s^{-1}}$. Define:

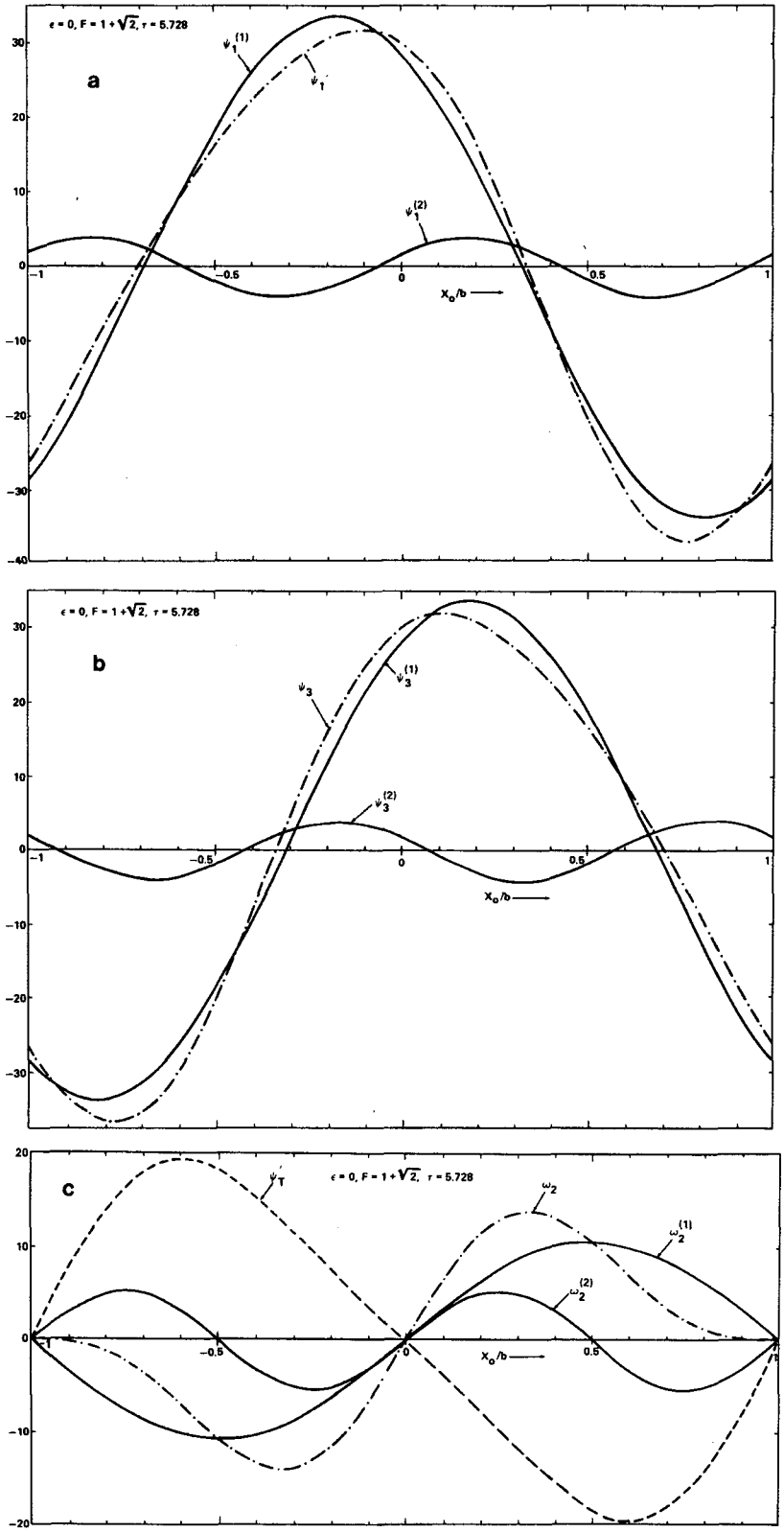


FIG. 1. (a) Dry case, $\epsilon = 0$, $F = 1 + \sqrt{2}$, $r = 5.728$. Upper level: $\psi_1^{(1)}$, first-order eddy streamfield; $\psi_1^{(2)}$, second-order eddy streamfield; $\psi'_1$, total eddy streamfield. Units: $B = S_d p_2 A_d (2f\bar{u}_T^{(0)}\lambda_d^{1/2})^{-1}$. (b) As in (a) except that the fields are at the lower level, indicated by subscript 3. (c) Dry case, $\epsilon = 0$, $F = 1 + \sqrt{2}$, $r = 5.728$. Vertical motion field $\omega$ ($=dp/dt$) and total eddy temperature field $\psi'_T$. Superscript (1): First-order eddy. Superscript (2): Second-order eddy. Prime: Total eddy. Subscript 2: Middle level. Unit for $\omega$'s = $A_d$. Unit for $\psi'_T$: $B$.

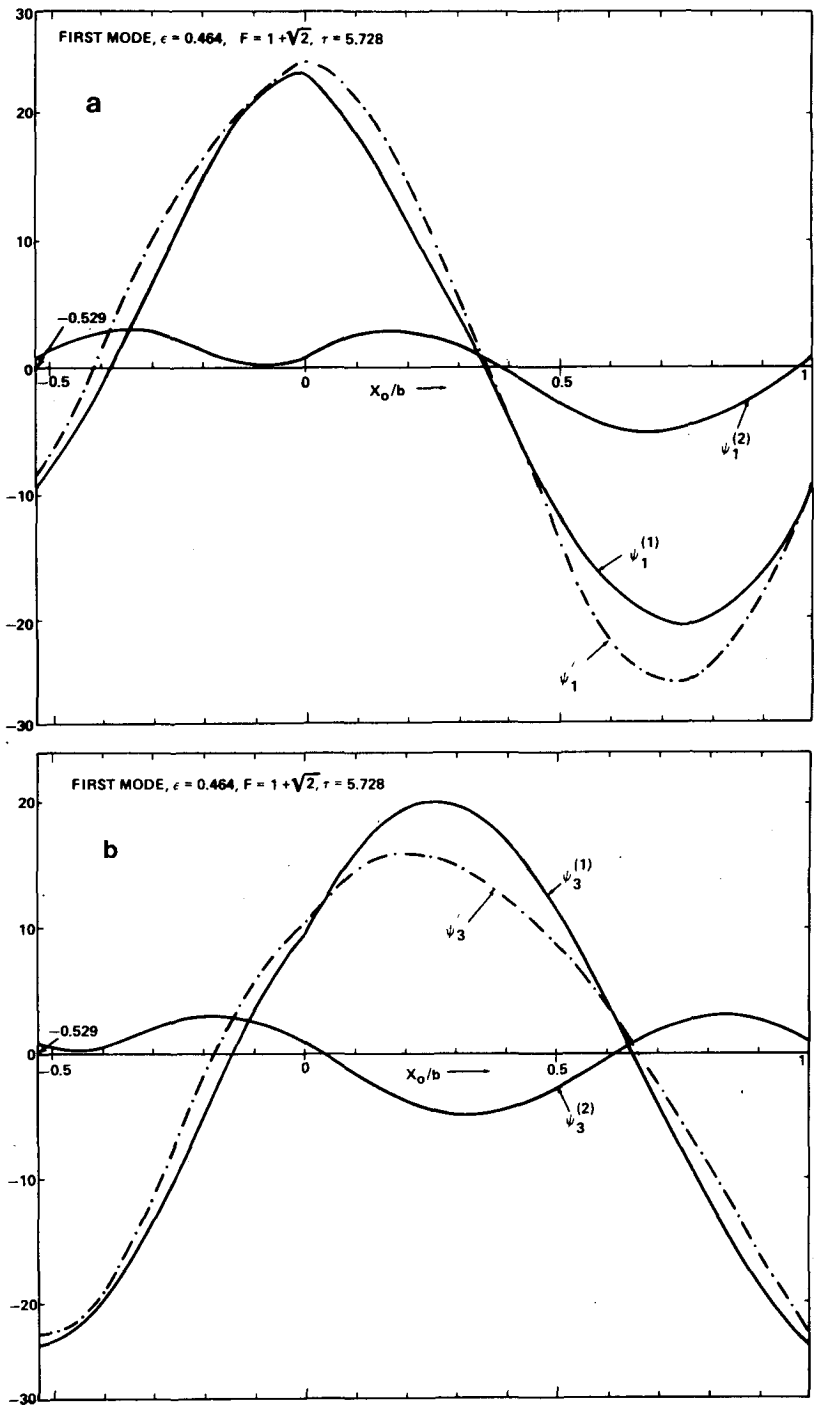


FIG. 2. As in Fig. 1 except for first mode, $\epsilon = 0.464$.

$$\tau = \lambda_d^{1/2} \bar{u}_T^{(0)} t_0, \tag{32}$$

where

$$\lambda_d = 2f^2/S_d p_2^2.$$

Substituting the prescribed parameters in the formulas for $\nu$, $A_m$, $\hat{\Omega}$, and $\tilde{\Omega}$ (not shown) with the aid of (32), the limiting time for $\epsilon = 0.464$ is

(i) First mode: $\tau = 5.728 \rightarrow t_0 = 4.749$ days,
(ii) Second mode: $\tau = 1.562 \rightarrow t_0 = 1.295$ days.

In order to see the differences and similarities in wave structure between the moist model and dry model, the wave structure in the dry model at $\tau = 5.728$ must be discussed. Fig. 1(a) (upper level)

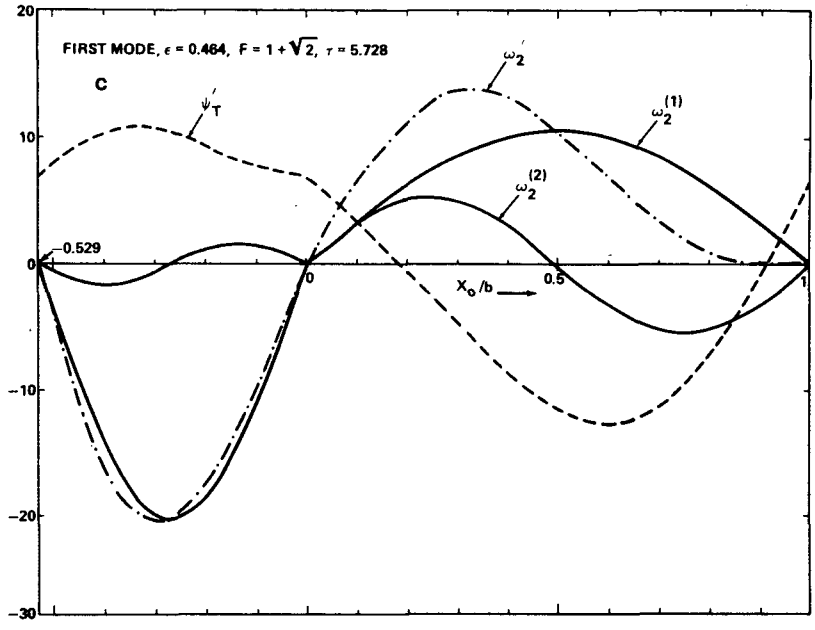


FIG. 2. (*Continued*)

and Fig. 1(b) (lower level) show the first order, second order, and total eddy streamfields. The effect of the second order eddy streamfield is to intensify and contract the trough and to weaken and diffuse the ridge of the total eddy streamfield and to shift the ridge slightly to the east and the trough slightly to the west at the upper level, but to shift the ridge slightly westward and the trough slightly eastward at the lower level. These features are explained also in a disturbance with meridional variation in ST (1972). This is mainly caused by the term due to the correlation between the vorticity and horizontal convergence in the vorticity equation. In the trough, the vorticity is positive and it is in the region of horizontal convergence; thus the generated vorticity is positive and it augments the original positive vorticity. In the ridge, the vorticity is negative and it is in the region of horizontal divergence; thus the generated vorticity is again positive, but the original vorticity is negative, so the absolute magnitude of the negative vorticity is reduced when they are added. Fig. 1(c) shows the vertical motion fields and the total eddy temperature field. Relatively strong temperature gradient on the east side of minimum temperature but relatively weak temperature gradient on the west side (cf. ST, 1974) are seen. The effect of the second order eddy vertical motion field is to make the total eddy vertical motion field asymmetric in each region so that the direct circulation is strong where temperature gradient is relatively weak and the direct circulation is relatively weak where the temperature gradient is strong.

The wave structure for the first mode, $\epsilon = 0.464$ at the limiting time $\tau = 5.728$, is discussed. At the upper level, the effect of the second order eddy streamfield is to intensify the trough substantially and also intensify the ridge slightly [cf. Fig. 2(a)]. But at the lower level the intensity of the ridge is reduced considerably and the trough is weakened slightly due to the second-order eddy streamfield [cf. Fig. 2(b)]. In Fig. 2(c), in the descending region the vertical motion fields are similar to the corresponding fields in the dry model, the warming has spread itself over parts of the sinking region near the interfaces due to the first order effect of eddy temperature field (cf. TF, 1983), but the nonquasi-geostrophic effect causes an asymmetry with eddy temperature field similar to the dry result discussed in the previous paragraph. However, the second-order eddy vertical motion field results in a slight westward shift of the maximum ascending motion with further asymmetry of the total eddy temperature field, i.e., a tendency of flattening of total eddy temperature profile on the east side of ascending region.

The wave structure of the second mode is shown in Figs. 3(a, b, c). It is seen that due to the second order eddy streamfield both trough and ridge are weakened slightly at the upper level [cf. Fig. 3(a)], while they are both intensified slightly at the lower level [cf. Fig. 3(b)]. Fig. 3(c) shows that the eddy temperature field is nearly symmetric in each region and the second order vertical motion field results in an eastward shift of the position of maximum ascending motion.

Due to the second-order vertical motion field, the position of maximum ascending motion shifts eastward in the dry model [cf. Fig. 1(c)], but it shifts slightly westward in the first mode of the moist model [cf. Fig. 2(c)]. In order to see the moisture effect on this feature,

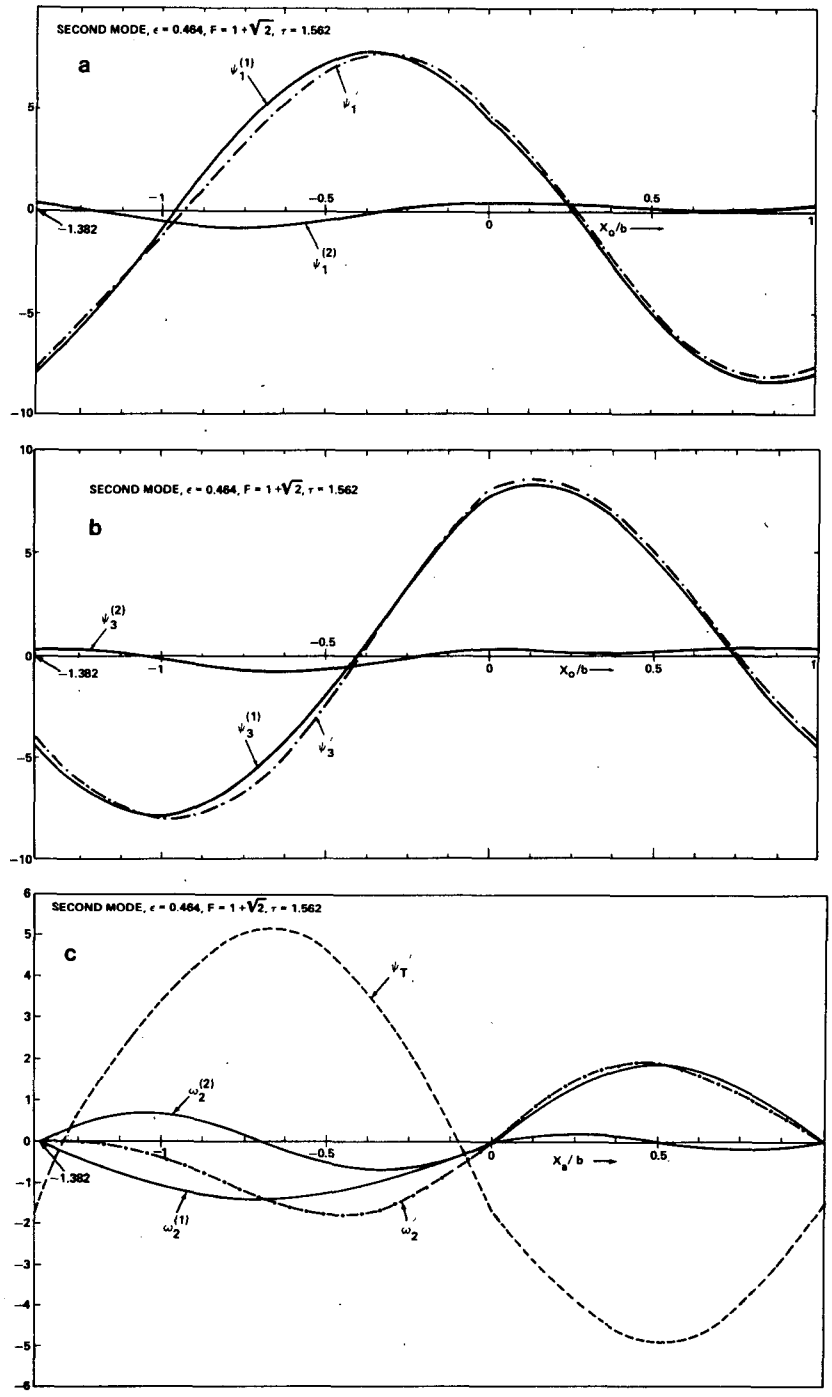


FIG. 3. As in Fig. 2 except for second mode.

the nondimensional amplitude of the second-order vertical motion field in the ascending region as a function of $\epsilon$ is shown in Fig. 4. The curve implies that for $0 \leqslant \epsilon < 0.305$, the position of maximum ascending motion shifts eastward due to the second order eddy vertical motion field, but it shifts westward for $0.305 < \epsilon < 1$. At $\epsilon = 0.305$ the second-order eddy vertical motion field vanishes in the ascending region. In contrast, for the second mode the position of maximum ascending motion shifts eastward for $0 \leqslant \epsilon < 1$ (cf. Fig. 5).

The zonal mean temperature $\bar{\psi}_T^{(1)}$, as a function of $F$ and $\epsilon$ for the first mode, is shown in Fig. 6 and for the second mode in Fig. 7. For both modes the max-

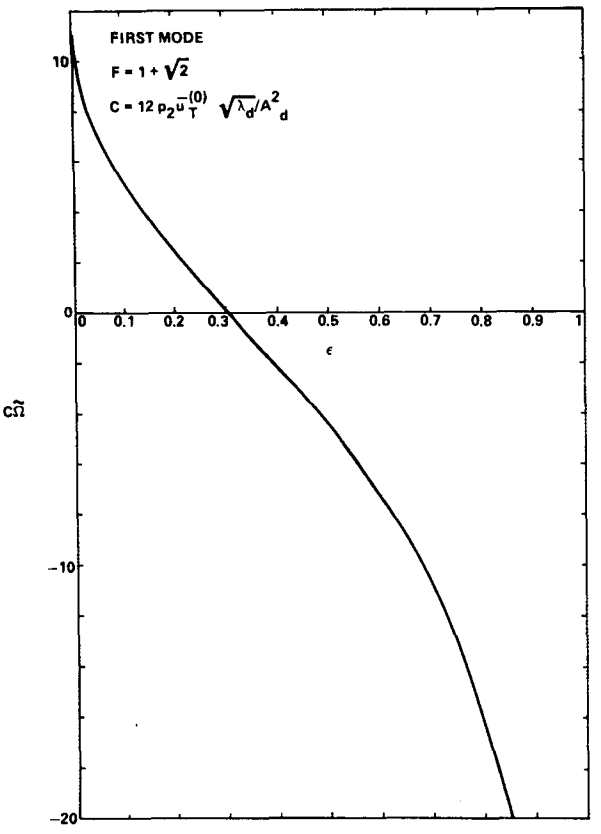


FIG. 4. Nondimensional amplitude of second-order eddy $\omega$ field as a function of $\epsilon$ for the first mode, $F = 1 + \sqrt{2}$.

imum mean temperature occurs for $F > 1 + \sqrt{2}$ and as $\epsilon$ increases the value of $F$ for maximum $\bar{\psi}_T^{(1)}$ decreases for the first mode and it increases for the second mode.

## 6. Energetics

To obtain the eddy kinetic energy equation, we multiply (16a) and (17a) by $\tilde{\psi}'_1$ and $\tilde{\psi}'_1$ respectively, multiply (16b) and (17b) by $\tilde{\psi}'_3$ and $\tilde{\psi}'_3$ respectively, and take the zonal average as defined by (8) and the sum. With the requirement for energetic consistency (Haltiner, 1971)

$$\overline{\psi'_1 H'_1} + \overline{\psi'_3 H'_3} = 0, \tag{33}$$

we obtain

$$\frac{\bar{u}_T^{(0)}\lambda_d^{1/2}}{S_d A_d^2}\frac{d}{dt_0}K' = -\frac{2f\bar{u}_T^{(0)}\lambda_d^{1/2}}{S_d p_2 A_d^2}\overline{\omega'_2\psi'_T}, \tag{34}$$

where the eddy kinetic energy is defined as

$$K' = \frac{1}{2}\left[\overline{\left(\frac{\partial\psi'_1}{\partial x_0}\right)^2 + \left(\frac{\partial\psi'_3}{\partial x_0}\right)^2}\right]. \tag{35}$$

To obtain the eddy available potential energy equation, we multiply (16c) and (17c) by $\tilde{\psi}'_T$ and $\tilde{\psi}'_T$ respectively, and take the zonal average using the definition (8). The result is

$$\frac{\bar{u}_T^{(0)}\lambda_d^{1/2}}{S_d A_d^2}\frac{d}{dt_0}A' = \frac{2f\bar{u}_T^{(0)}\lambda_d^{1/2}}{S_d p_2 A_d^2} \times\left[\overline{\omega'_2\psi'_T} + \frac{2f}{S_d p_2}\bar{u}_T^{(0)}\overline{v'_2\psi'_T} - \frac{\epsilon}{(a+b)} \times\int_{-a}^{0}\tilde{\omega}'_2\tilde{\psi}'_T dx_0\right], \tag{36}$$

where the eddy available potential energy is defined as

$$A' = \frac{2f^2}{S_d p_2^2}\overline{(\psi'_T)^2}. \tag{37}$$

Equations (34) and (36) are the same as those in TF except now the perturbation consists of both first-order and second-order variables. The following orthogonal relations can be shown:

$$\left.\begin{aligned}&\overline{\omega_2^{(1)}\psi_T^{(2)}} = \overline{\omega_2^{(2)}\psi_T^{(1)}} = 0\\ &\overline{v_{\psi_2}^{(1)}\psi_T^{(2)}} = \overline{v_{\psi_2}^{(2)}\psi_T^{(1)}} = 0\\ &\int_{-a}^{0}\tilde{\omega}_2^{(1)}\tilde{\psi}_T^{(2)}dx_0 = \int_{-a}^{0}\tilde{\omega}_2^{(2)}\tilde{\psi}_T^{(1)}dx_0 = 0\end{aligned}\right\}. \tag{38}$$

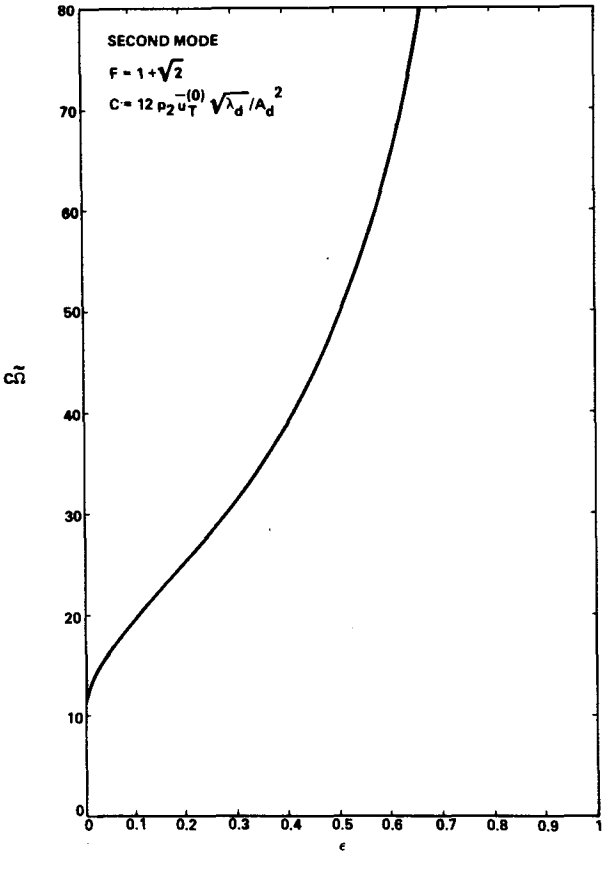


FIG. 5. As in Fig. 4 except for the second mode.

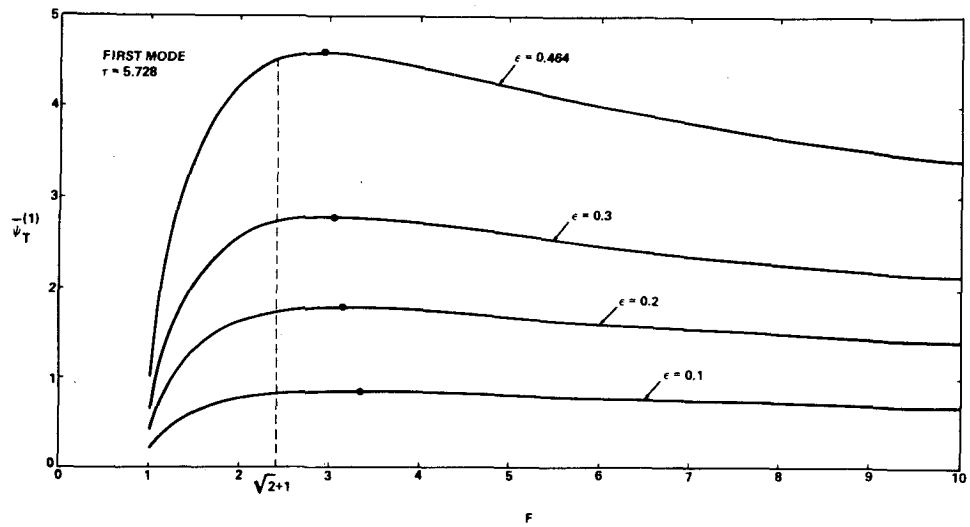


FIG. 6. The zonally-averaged first-order temperature field $\bar{\psi}_T^{(1)}$ (in the unit of $B$) as a function of $F$ for $\epsilon = 0.1$, 0.2, 0.3 and 0.464, for first mode at $\tau = 5.728$.

Thus, using (109) we have

$$\left.\begin{aligned}\overline{\omega_2'\psi_T'} &= \overline{\omega_2^{(1)}\psi_T^{(1)}} + \overline{\omega_2^{(2)}\psi_T^{(2)}}\\ \overline{v_{\psi_2}'\psi_T'} &= \overline{v_{\psi_2}^{(1)}\psi_T^{(1)}} + \overline{v_{\psi_2}^{(2)}\psi_T^{(2)}}\\ \int_{-a}^{0}\tilde{\omega}_2'\tilde{\psi}_T' dx_0 &= \int_{-a}^{0}\tilde{\omega}_2^{(1)}\tilde{\psi}_T^{(1)} dx_0\\ &\quad + \int_{-a}^{0}\tilde{\omega}_2^{(2)}\tilde{\psi}_T^{(2)} dx_0\end{aligned}\right\}. \quad (39)$$

The heat transport formulas involving the first-order eddy are the same as those in TF. With appropriate constant factors multiplied [as it is evident on the right side of (36)], (39) can be expressed with the abbreviated symbols as follows:

$$\left.\begin{aligned}\text{VTS} &= \text{VT1} + \text{VT2}\\ \text{HTS} &= \text{HT1} + \text{HT2}\\ \text{MTS} &= \text{MT1} + \text{MT2}\end{aligned}\right\}. \quad (40)$$

The left side of (36) is denoted as $d(\text{APES})/dt_0$, the temporal variation of total eddy available potential energy. Thus

$$d(\text{APES})/dt_0 = \text{VTS} + \text{HTS} + \text{MTS}. \quad (41)$$

Similarly, the temporal variation of eddy available potential energy due to the first order eddy

$$d(\text{APE1})/dt_0 = \text{VT1} + \text{HT1} + \text{MT1}. \quad (42)$$

The energetics of the waves for the typical atmospheric parameters listed in Section 8 are now discussed.

Figure 8 shows the nondimensional transports for the dry model $a = b$ and $r = 5.728$. For $F$ from 1 to 5.6, the second-order heat transports are opposite in sign to the corresponding first-order heat transports and their magnitudes are small. The difference between the generation of total eddy available potential energy and the generation of eddy available potential energy

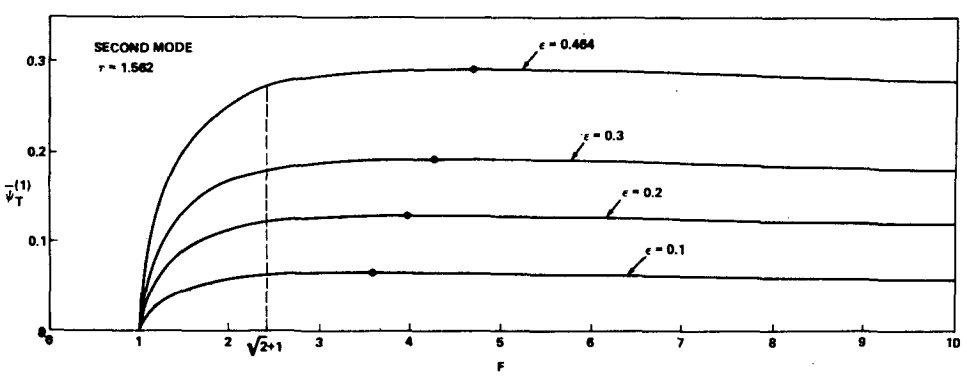


FIG. 7. As in Fig. 6 except for second mode at $\tau = 1.562$.

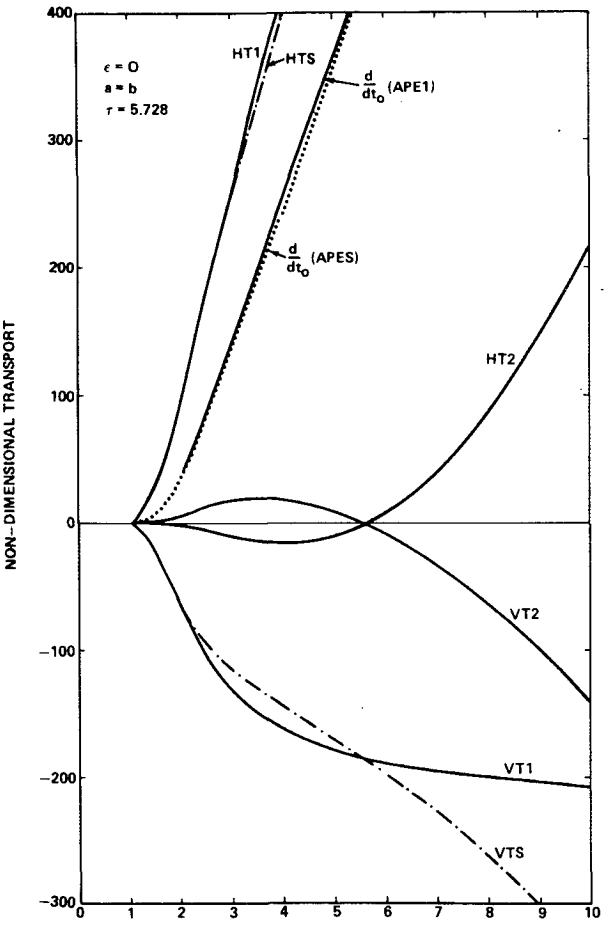


FIG. 8. Nondimensional transports as functions of $F$ for dry model ($\epsilon = 0$), $a = b$, $\tau = 5.728$. HT1: Meridional heat transport due to first-order eddy. HT2: Meridional heat transport due to second-order eddy. HTS: Sum of HT1 and HT2. VT1: Vertical heat transport due to first-order eddy. VT2: Vertical heat transport due to second-order eddy. VTS: Sum of VT1 and VT2. APE1: Eddy available potential energy due to first-order eddy. APES: Sum of eddy available potential energy due to first-order eddy and that due to second-order eddy.

due to the first-order eddy is extremely small for this range of $F$. In Fig. 9 is shown the nondimensional transports for the first mode, $\epsilon = 0.464$ and $\tau = 5.728$. All transport quantities except for MT1 are smaller in magnitude than the corresponding ones in the dry model. In comparison with the dry model, although positive MT1 exists in the first moist mode, due to the drastic reduction of HT1 the generation of eddy available potential energy for either total eddy or first-order eddy is much less than that in the dry model. The transport quantities due to the second-order eddy become appreciable for $F > 6$. MT2 is not shown in Fig. 9 because its magnitudes are extremely small. Fig. 10 shows the nondimensional transports for the second mode, $\epsilon = 0.464$, $\tau = 1.562$. We note that the changes are small. It is a result of the short time limit.

Now we fix $F = 1 + \sqrt{2}$ and examine how the transport quantities vary with $\epsilon$. Fig. 11 shows the nondimensional transports for the first mode. The changes due to the second-order eddy are small and nearly uniform as $\epsilon$ increases from zero to unity. Fig. 12 shows the nondimensional transports for the second mode. The effects due to the second-order eddy are small for small $\epsilon$. But the effects become significant for $\epsilon > 0.7$ and VT2 approaches VT1 as $\epsilon$ approaches 0.9. Thus the expansion is invalid for $\epsilon \geqslant 0.9$.

## 7. Conclusion

The non-quasi-geostrophic effects in baroclinic waves in a saturated atmosphere with vertical motion subject to pseudo-adiabatic processes have been studied. For the dry model the non-quasi-geostrophic effects appear in the intensification and contraction of the trough of the streamfield and the weakening and diffusion of the ridge of the steamfield both at the upper level and lower level. But for the first mode in the

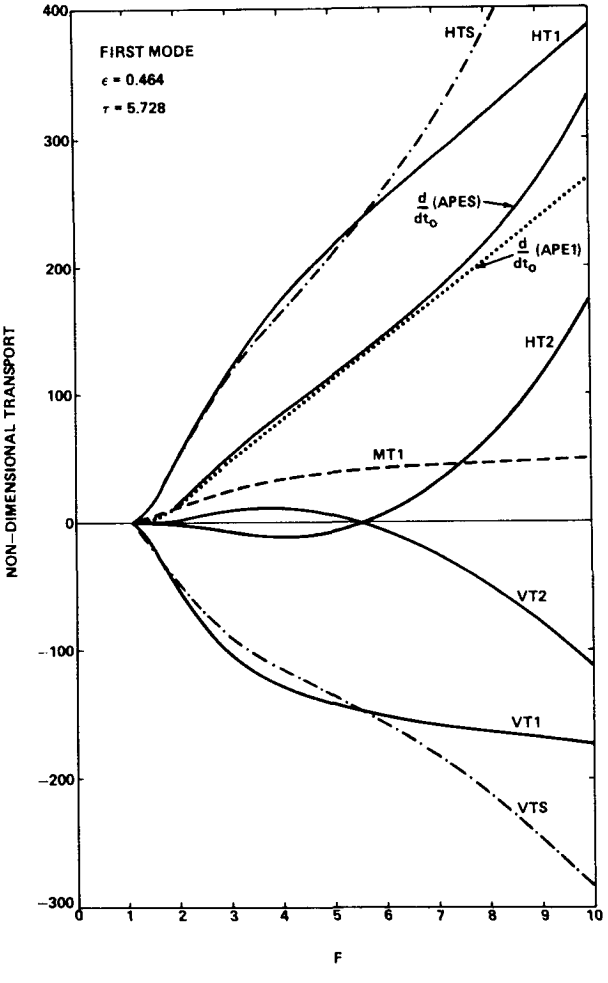


FIG. 9. As in Fig. 8 except for first mode, $\epsilon = 0.464$ and dashed curve MT1 (direct moisture transport due to first-order eddy).

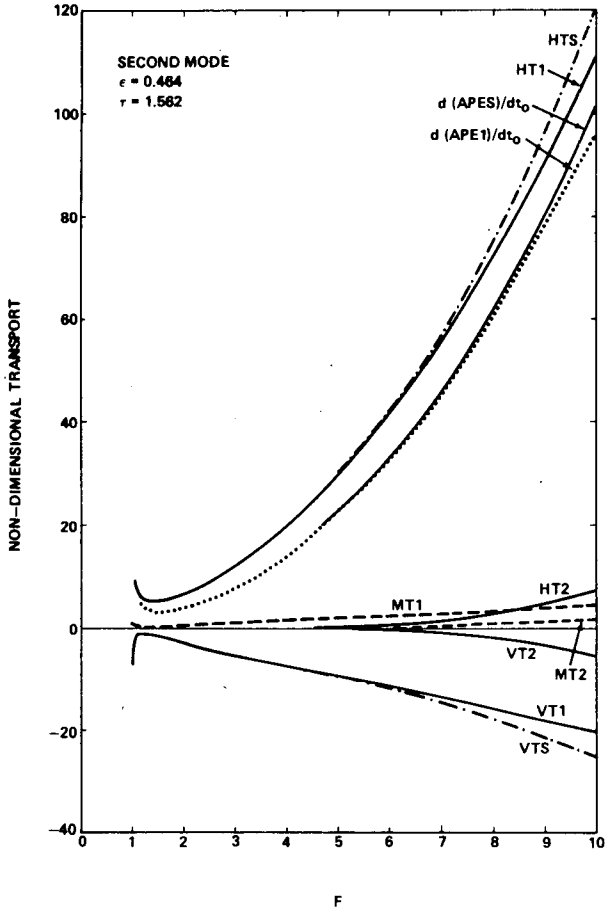


FIG. 10. As in Fig. 9 except for second mode, $\tau = 1.562$, and MT2 (direct moisture transport due to second-order eddy).

moist model, due to the non-quasi-geostrophic effects, both trough and ridge are intensified at the upper level with stronger intensification of the trough, and are weakened at the lower level with considerable weakening of the ridge. The feature of the formation of the frontal zone on the east side of the descending region compared to the weakening temperature gradient on the west side is similar to that in the dry model. The total vertical motion field becomes asymmetric in each region and the profile of the eddy temperature field in the ascending region becomes more subtle, i.e., there is an inflection point in the profile. For the second mode, due to the non-quasi-geostrophic effects, both trough and ridge are weakened at the upper level, but they are intensified at the lower level. The temperature profile in each region becomes nearly symmetric.

The main characteristics of the energetics for the first-order solution have been discussed in TF. It is noted that for the dry mode ($a = b$) and first moist mode ($\epsilon = 0.464$), the heat transport quantities due to the second-order eddy are small and opposite in sign compared to their respective transports due to the first order eddy for $1 < F < 5.6$. For $F > 5.6$ the sign changes and the magnitudes become larger, especially for $F$ near and greater than 10 (cf. Figs. 8 and 9). For the wave of maximum growth rate, the transport quantities due to the second-order eddy are small compared to their respective transports due to the first-order eddy for $\epsilon$ varying from 0 to 1 for the first mode. However, for the second mode, the transport quantities due to the second-order eddy become comparable to their respective transport quantities due to the first-order eddy for $0.9 < \epsilon < 1$ that the expansion of the variables is invalid for this range of $\epsilon$.

For the first moist mode, the feature of the intensification of both the trough and ridge at the upper level [cf. Fig. 2(a)] and the weakening of both ridge and trough at the lower level [cf. Fig. 2(b)] due to the non-quasi-geostrophic effects seems to imply the increase of the ratio of eddy kinetic energy at the upper level to that at the lower level compared to the eddy kinetic energy ratio in the moist quasi-geostrophic model, provided the discontinuity of the slope of the streamfield at the interface is disregarded. For the dry model [cf. Figs. 1(a), (b)], the implication is that this

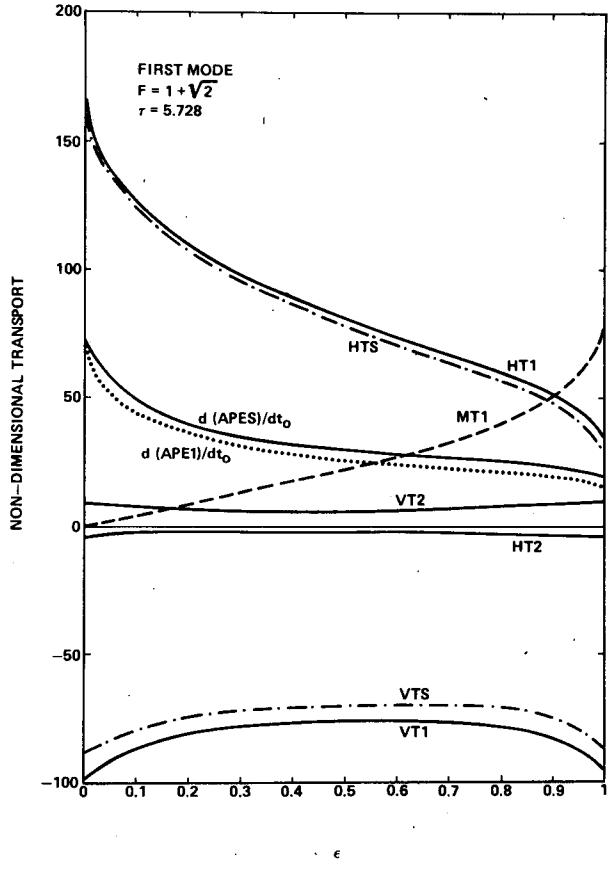


FIG. 11. Nondimensional transports as functions of $\epsilon$ for first mode, $F = 1 + \sqrt{2}$, $\tau = 5.728$. Other symbols are the same as those in Fig. 9.

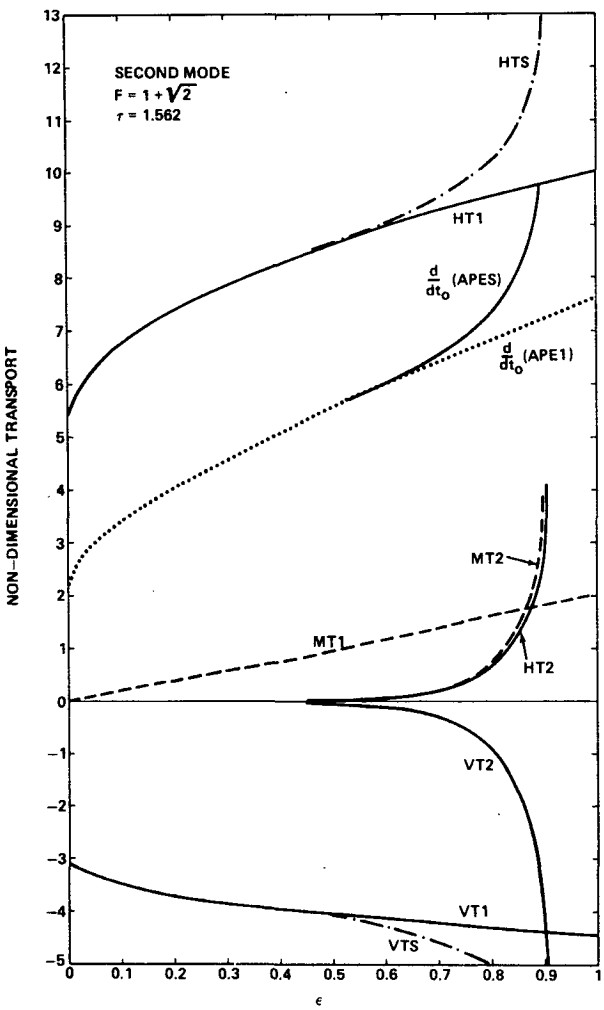


FIG. 12. Nondimensional transports as functions of $\epsilon$ for second mode, $F = 1 + \sqrt{2}$, $\tau = 1.562$. Other symbols are the same as those in Fig. 10.

ratio would not change significantly due to the non-quasi-geostrophic effects. Thus, a manifestation of latent heat release in non-quasi-geostrophic terms seems to increase the ratio of the eddy kinetic energy at the upper level to that at the lower level. This seems to be consistent with Gall (1976) in which he showed that the effects of latent heat release tended to develop a maximum eddy kinetic energy at the middle or upper level more rapidly.

The non-quasi-geostrophic effects make the vertical motion field asymmetric in each region. These effects in moist baroclinic waves tend to smooth out the discontinuity in the slope of vertical motion field at the interface between the descending region to the east and ascending region to the west, but may enhance the discontinuity at the interface with ascending region to the east and descending region to the west.

In this paper, the non-quasi-geostrophic effects enter only as nonlinear terms. The model neglects other nonlinear effects. For example, the increase in static stability as the wave develops has not been considered. This effect tends to reduce the growth rate and the vertical tilt of the wave in time for ST model excluding latent heat release (cf. ST, 1982; Tang, 1980). Presumably, these would be modified if the latent heat release were included. Petterssen *et al.* (1962) considered two types of mid-latitude cyclones. Cyclones over the North American continent tended to have the vertical tilt reduced as they evolved; on the other hand, the cyclones over the North Atlantic tended to maintain their vertical tilts. The difference can be attributed to the pronounced diabatic heating, especially the latent heat release, in the North Atlantic. Recently, Chang *et al.* (1982) made a numerical case study on the effects of latent heat release on a developing cyclone. They found that in a weakly baroclinic system, the wet simulation successfully reproduced the closed circulation throughout the troposphere and the latent heat release stabilized the lower troposphere and reduced the horizontal temperature gradient. The increase of static stability due to the latent heat release was because of pronounced heating in the middle and upper troposphere. Thus, there was a strong increase in static stability in the lower troposphere. In contrast, our model is a two-level model which has only one temperature level, i.e., the middle level, and our perturbation has no meridional variation. In our formulation, the static stability in the dry region and the lower static stability in the moist region are prescribed, thus the increase of zonal mean temperature due to latent heat release is uniform in the vertical. Hence our model can not reproduce the increase of static stability with time as in Chang *et al.*

As in TF, the moisture transport term in the eddy available potential energy equation is small compared to other terms individually in the energetics calculation for cyclone-scale motion which is consistent with the observational results of Smith (1980) and the numerical results of Hayashi and Golder (1981) that the condensational heating contributes very little to the energetics of extratropical cyclones.

The modification of the moisture field by the growing wave has not been investigated in this paper. The modification of the moisture field by the wind field and temperature field was investigated numerically by Williams *et al.* (1981; hereafter referred to as WCC) for the condensation effect and the surface motion effect on the structure of steady-state fronts. Their initial wind field and temperature field looked very much like a realistic portion of a finite-amplitude baroclinic wave (Williams, 1972, 1974; WCC). The effect of latent heat release on the strength of frontal zones in our paper can be demonstrated as follows. Similar to WCC, the measure of the width of the frontal zone is defined as

$$d = \frac{\psi'_{T\max} - \psi'_{T\min}}{|\partial\psi'_T/\partial x_0|_{\max}}, \tag{43}$$

where the discontinuity of $\partial\psi'_T/\partial x_0$ across the interface for the moist model is ignored. From the parameters given in Section 5, $b = 2800$ km. Using (43), the values of $d$ are calculated. They are

First moist mode:

$$d = 0.271b = 759 \text{ km}, \tag{44a}$$

Dry mode:

$$d = 0.391b = 1095 \text{ km}. \tag{44b}$$

These values are very close to those in the midtroposphere in WCC. Comparing (44a) and (44b), it is concluded that the frontal zones are strengthened by the condensation heating—the same conclusion as that above the planetary boundary layer in WCC.

*Acknowledgments.* We thank Mr. John Theon, manager of NASA Global Weather Program, for support of this research, which was supported in part by NASA Contract NAS8-34010.

## REFERENCES

Chang, C. B., D. J. Perkey and C. W. Kreitzberg, 1982: A numerical case study of the effects of latent heating on a developing wave cyclone. *J. Atmos. Sci.*, **39,** 1555–1570.

Gall, R., 1976: The effects of released latent heat in growing baroclinic waves. *J. Atmos. Sci.*, **33,** 1686–1701.

Haltiner, G. J., 1971: *Numerical Weather Prediction.* Wiley and Sons, 317 pp.

Hayashi, Y., and D. G. Golder, 1981: The effects of condensational heating on midlatitude transient waves in their mature stage: Control experiments with a GFDL general circulation model. *J. Atmos. Sci.*, **38,** 2532–2539.

Holton, J. R., 1972: *An Introduction to Dynamic Meteorology.* Academic Press, 319 pp.

Petterssen, S., D. L. Bradbury and K. Pedersen, 1962: The Norwegian cyclone models in relation to heat and cold sources. *Geofys. Publ.*, **24,** 243–280.

Phillips, N., 1954: Energy transformations and meridional circulations associated with simple baroclinic waves in two-level quasi-geostrophic model. *Tellus,* **6,** 273–286.

Saltzman, B., and C-M. Tang, 1972: Analytical study of the evolution of an amplifying baroclinic wave. *J. Atmos. Sci.*, **29,** 427–444.

——, and ——, 1974: Mid-tropospheric frontogenesis in an amplifying baroclinic wave. *J. Atmos. Sci.*, **31,** 835–839.

——, and ——, 1975: Analytical study of the evolution of an amplifying baroclinic wave. Part 2: Vertical motion and transport properties. *J. Atmos. Sci.*, **32,** 243–259.

——, and ——, 1982: A review of some analytical studies of finite amplitude baroclinic waves, including a new algorithm for the saturation effects of static stability and baroclinicity variations. *J. Meteor. Soc. Japan,* **60,** 1–15.

Smith, P. J., 1980: The energetics of extratropical cyclones. *Rev. Geophys. Space Phys.*, **18,** 378–386.

Tang, C-M., 1980: The influence of the time change of static stability and wind shear on baroclinic waves. *Pure Appl. Geophys.*, **118,** 706–719.

——, and G. H. Fichtl, 1983: The role of latent heat release in baroclinic waves. *J. Atmos. Sci.*, **40,** 53–72.

Williams, R. T., 1972: Quasi-geostrophic versus non-geostrophic frontogenesis. *J. Atmos. Sci.*, **29,** 3–10.

——, 1974: Numerical simulation of steady-state fronts. *J. Atmos. Sci.*, **31,** 1286–1296.

——, L. C. Chou, and C. J. Cornelius, 1981: Effects of condensation and surface motion on the structure of steady-state fronts. *J. Atmos. Sci.*, **38,** 2365–2376.